

Methods and Applications

A New Approach Refined Probabilistic Health Risk Assessment of Shaoguan Smelter Based on Microenvironment — Guangdong Province, China, 2021

Liangzhong Li^{1,2}; Lei Zhang^{2,3,4}; Yile Yan²; Bingbing Sun²; Ruixue Ma²; Qiong Wang^{5,#}; Yunjiang Yu²; Haoran Yuan¹; Jing Cao³

ABSTRACT

Introduction: This study introduces a novel method for developing an advanced exposure conceptual model tailored for health risk assessment, focusing on microenvironments.

Methods: The research was conducted at a major smelter in China to assess the health risks associated with trace metals (TMs) pollutants in the facility and the surrounding soil.

Results: Deterministic risk assessment indicated that cobalt, cadmium, antimony, manganese, arsenic, plumbum, and mercury (Co, Cd, Sb, Mn, As, Pb, and Hg) necessitated further evaluation through probabilistic risk assessment to assess potential health risks to residents. The 95% quantile concentrations of other TMs were found to be within acceptable health risk limits. For the probabilistic risk assessment, exposure parameters such as body weight, respiration rate, and exposure duration were collected using a questionnaire. This targeted assessment of the residential microenvironment revealed it as the site of the highest carcinogenic (CR) and non-carcinogenic risks (NCR), with values ranging from 2.84×10^{-5} to 6.7×10^{-5} and 1.59 to 5.57, respectively.

Conclusion: The primary contaminants posing the greatest health risks in residential and industrial areas have been identified as As, Pb, and Mn. The probabilistic health risk model, which focuses on microenvironmental factors, yields more precise results and offers a valuable tool for managing soil health risks.

The human health risk assessment model serves as an essential tool for evaluating the risks associated with environmental pollutants (1). Historically, most studies employed deterministic methods, calculating health

risks based predominantly on concentrations of total soil trace metals (TMs) and setting exposure parameters (2–3). Nevertheless, variabilities such as the daily intake rate of toxins, body weight of the population, duration and frequency of exposure among individuals in the study area introduce uncertainties that can compromise the precision of risk assessment outcomes (4). To address these uncertainties, probabilistic analysis methods are often applied (5), with Monte Carlo simulation being the most popular technique. This method involves generating random numbers for iterative calculations across different distributions, presenting results as probability distributions. Consequently, it allows for the estimation of the probability that the risk associated with each heavy metal exceeds established guideline values (6).

Previously, research into the health risks posed by pollutants concentrated on broad geographic regions, often neglecting the full spectrum of potential exposure scenarios (7), which could notably influence the results of risk assessments (8). Consequently, this study employs a smelter and its immediate vicinity as a case study area to develop a refined probabilistic health risk assessment tailored to microenvironments, aiming to enhance the accuracy of these assessments.

METHODS

Study Area and Sample Collection

The smelter, located in Guangdong Province and established in 1966, produces electric lead, refined zinc, cadmium, and mercury. It has an annual capacity of 350,000 tons, making it the third-largest smelter in China (Figure 1) (9).

Land use type plays a critical role in assessing the health risks associated with land. Utilizing satellite images from the Google Maps service (2018), our study area was categorized into four primary land use

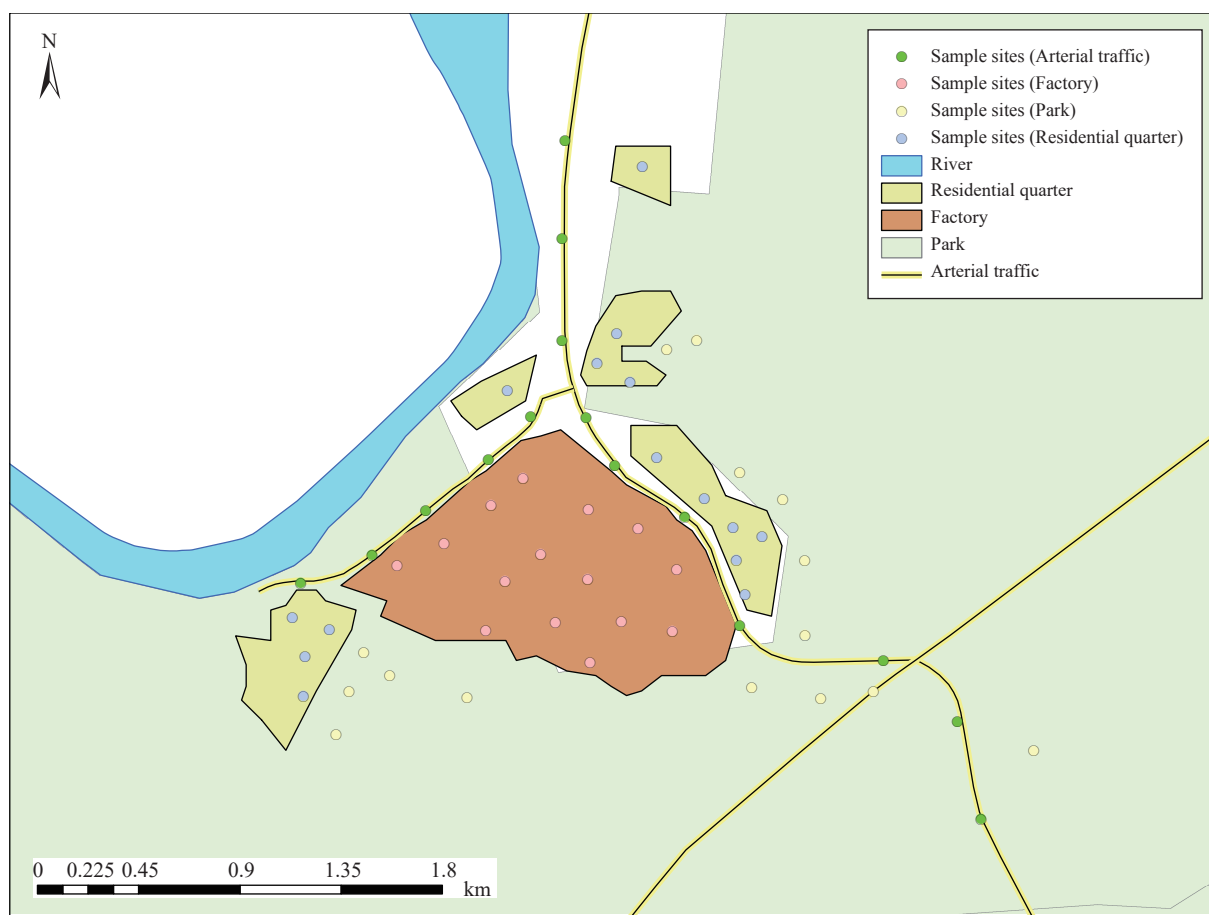


FIGURE 1. Location and sampling sites within the study area.

types: 1) factory area, 2) residential area, 3) transportation area (T), and 4) park (P). This research comprehensively evaluated the contamination levels of 16 heavy metals — beryllium, chromium, manganese, cobalt, nickel, copper, zinc, arsenic, molybdenum, silver, tin, antimony, thallium, plumbum, cadmium, and mercury (Be, Cr, Mn, Co, Ni, Cu, Zn, As, Mo, Ag, Sn, Sb, Tl, Pb, Cd, and Hg) in both plant life and surrounding soils, resulting in the collection of 60 samples, with 15 samples from each specified microenvironment (10). The geographic coordinates of all sample sites were precisely documented using handheld Global Positioning System (GPS) devices (Figure 1). Following the protocol outlined in GB/T 36197-201, each representative soil sample, obtained from the top 10 cm, constituted a composite of five sub-samples collected from a minimum spacing of 1 m at each site. After the exclusion of large stones and grassroots, the initial weight of each sample was ensured to be no less than 1 kg. All samples were preserved in polyethylene bags and transported to the laboratory for detailed analysis.

Soil Sample Analysis

In the laboratory, soil samples were initially dried in a cool, ventilated area and sieved using a 100 mesh screen. Subsequently, these samples were digested employing the $\text{HNO}_3\text{-HClO}_4\text{-HF}$ method and stored in amber glass vials. As and Hg concentrations were quantified using an atomic fluorescence spectrometer (AFS-8220, Beijing Titan Instruments, China), while concentrations of other TM were measured with an inductively coupled plasma mass spectrometer (ICP-MS Agilent 7900) (11). For As and Hg, analysis and quality assurance/quality control (QA/QC) procedures followed the HJ 680 standard (12), and for other TMs, the USEPA 6020B method (USEPA, 2014b) was used.

Questionnaire Survey

A total of 487 questionnaires were administered at the study site, categorized by age into adults (ages over 18 years, $n=238$) and children (ages under 18 years, $n=249$). The participants, all permanent residents living within 5 km of the smelter for at least six months, included children under 8 years whose

questionnaires were completed by their parents. The questionnaire comprised two sections: the first section gathered basic demographic and physical data such as gender, age, height, and weight; the second involved a 24-hour time-activity pattern survey that classified respondent's time spent across four distinct microenvironments (13). Data collection was conducted through face-to-face interviews, during which responses were directly recorded by the interviewer.

Health Risk Assessment Model and Monte Carlo Simulation

Human health risks, encompassing both carcinogenic (CR) and non-carcinogenic risks (NCR), were evaluated for two distinct groups: adults and children. The detailed health risk assessment model can be found in Supplementary Material (available at <https://weekly.chinacdc.cn/>).

In this study, we utilized the Monte Carlo simulation as a probabilistic method to evaluate health risks. Input variables, including C, EF, ET, IR, and BW, were modeled using specific probability distribution functions derived from field investigation results. Due to the scarcity of sufficient toxicological data for each heavy metal, the RfD and SF were modeled as point estimates (Supplementary Table S1, available at <https://weekly.chinacdc.cn/>). To enhance the reliability of the findings, we performed 10,000 random iterations for each input variable during the simulations. The mean values and 95th percentiles of NCR and CR, calculated from the probabilistic outputs, were used to assess the health risks associated with multiple heavy metals (14–15).

Statistical Analysis

Statistical analysis was performed using SPSS Statistics (version 22.0; IBM Corp., Armonk, NY, USA). Distribution tests and charting were conducted using Origin (version 2019; Origin Lab Corp., Northampton, MA, USA). The Monte Carlo simulation was executed with Crystal Ball Software (version 11.1; Oracle Inc., Oracle, CA, USA).

RESULTS

Concentration-oriented Deterministic Health Risk Assessment

A deterministic risk assessment was conducted at 60

sampling sites within the study area to evaluate both CR and NCR (Supplementary Tables S2–S3, available at <https://weekly.chinacdc.cn/>). The health risk levels at the 95% quantile for TMs including Be, Cr, Ni, Cu, Mo, Zn, Ag, and Sn were found to be within the acceptable risk thresholds for cancer and non-carcinogenic effects in both adults and children (Figure 2).

However, chronic exposure to other TMs in sensitive populations is associated with a significant CR. The median CR values for Co and As and the 95% quantiles for Cd and Pb in adults exceeded the US EPA recommended threshold of 1×10^{-6} (Figure 2A). In children, the median values for Co, As, and Pb and the 95% quantiles for Cd surpassed acceptable risk levels, with the 95% CR for As and Pb exceeding 1×10^{-4} . Therefore, further probabilistic analysis is essential to accurately assess the risks associated with exposure to Co, As, Cd, and Pb (Figure 2B).

Regarding the NCR from population exposure, the median risk for Mn in adults was 2.77, surpassing the level recommended by the US EPA (NCR=1). Additionally, the 95th percentile values for As and Cd were 8.17 and 1.09, respectively, both exceeding established threshold values (Figure 2C). Median levels of Mn and As, along with the 95th percentile levels for Cd, Sb, and Hg in children, also surpassed the acceptable risk thresholds. Consequently, further analysis is warranted for the risks associated with Mn, As, Cd, Sb, and Hg. Ultimately, a probabilistic risk assessment is essential to ascertain the potential risks to residents from Co, Cd, Sb, Mn, As, Pb, and Hg (Figure 2D).

Probabilistic Exposure Assessment

In this study, we collected data on height, weight, and age of the exposed local population through a questionnaire survey and derived the probability distribution of exposure parameters and pollutant concentrations using Monte Carlo simulation (Supplementary Tables S4–S5, available at <https://weekly.chinacdc.cn/>). For assessing population health risks across various microenvironments, exposure time (ET) was defined as the duration spent daily by sensitive populations in these different settings (Supplementary Table S6, available at <https://weekly.chinacdc.cn/>). Based on the questionnaire results, ET was modeled using a triangular distribution.

The probability distribution of the total carcinogenic risk (TCR) associated with TMs across various

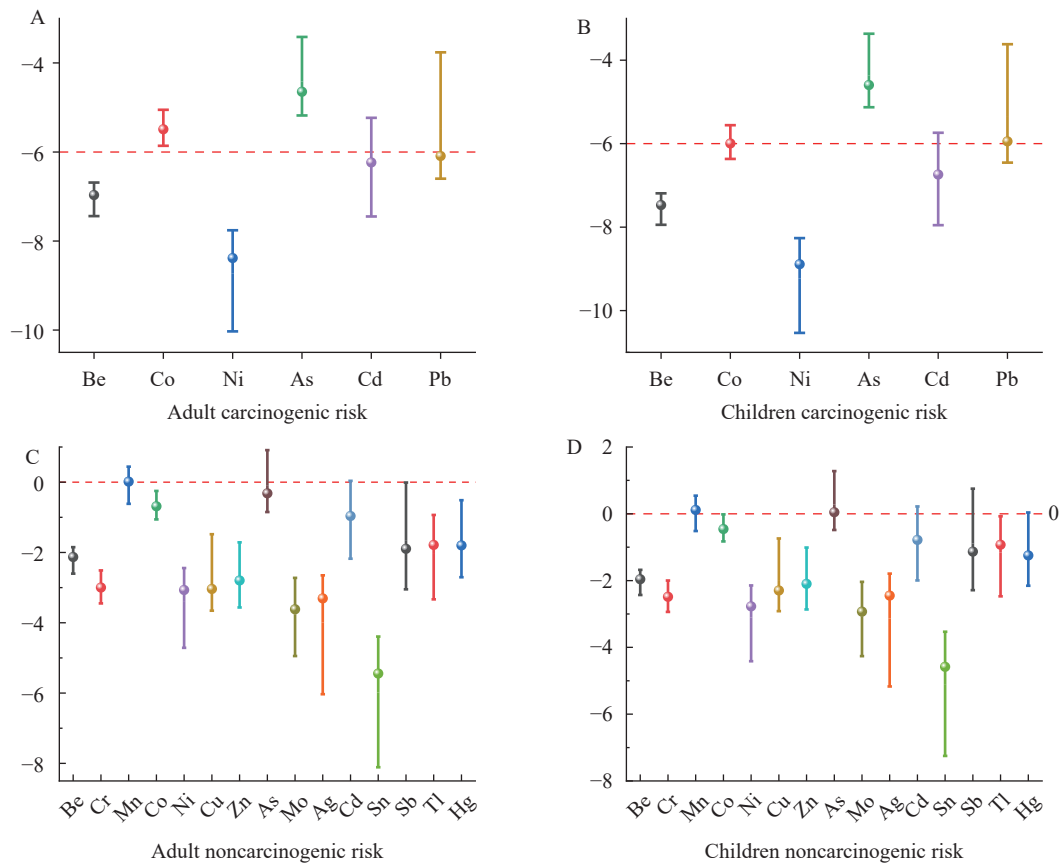


FIGURE 2. Deterministic risk assessment plotted on a logarithmic scale (base 10). (A) Adult carcinogenic risk; (B) Children carcinogenic risk; (C) Adult non-carcinogenic risk; (D) Children non-carcinogenic risk.

Note: The whiskers indicate deterministic risk outcomes at the 5% and 95% quantile concentrations at sampling points, while the dots correspond to deterministic risk outcomes at median concentrations.

microenvironments was analyzed (Figure 3). Details on the CR for specific TMs within each microenvironment are available in the supplementary data (Supplementary Figures S1–S4, available at <https://weekly.chinaccdc.cn/>). The average CR for adults demonstrated the highest values in residential areas (2.84×10^{-5}), followed by factories (1.74×10^{-5}), parks (3.43×10^{-6}), and traffic arteries (3.27×10^{-6}). For children, residential areas also showed the highest CR (6.7×10^{-5}), then traffic arteries (6.2×10^{-6}), and parks (3.52×10^{-6}). The likelihood of CR exceeding 1×10^{-6} for both adults and children ranged from 60% to 72% in parks and traffic arteries (Figures 3B–3C), while in residential and factory settings, this probability was approximately 95% (Figures 3A and 3D). As and Pb were identified as having the highest CR in each studied microenvironment (Supplementary Figures S1–S4).

The probability distribution of the total non-carcinogenic risk (TNCR) associated with TMs in various microenvironments was calculated as shown in

Figure 4. Detailed assessments of specific TMs in individual microenvironments can be found in Supplementary Figures S5–S8 (available at <https://weekly.chinaccdc.cn/>). The average NCR for adults was highest in residential areas (1.59), followed by factories (1.17), parks (0.35), and traffic arteries (0.21). For children, the risks were most severe in residential areas (5.57), then traffic arteries (0.74), and parks (0.59). The 95% quantile for adult NCR in park and traffic environments was below 1, indicating minimal health risks; however, the probability that children's average NCR exceeded 1 was 14% and 19.5%, respectively (Figure 4B and 4C). Within the factory environment, 44.35% of workers faced a NCR greater than 1 (Figure 4A). In residential settings, the probabilities of NCRs exceeding 1 for adults and children were 68.2% and 91.8%, respectively (Figure 4D). As and Mn presented the highest NCRs across all studied microenvironments (Supplementary Figures S5–S8).

Generally, to minimize restoration costs, priority regions and main contaminants for remediation in

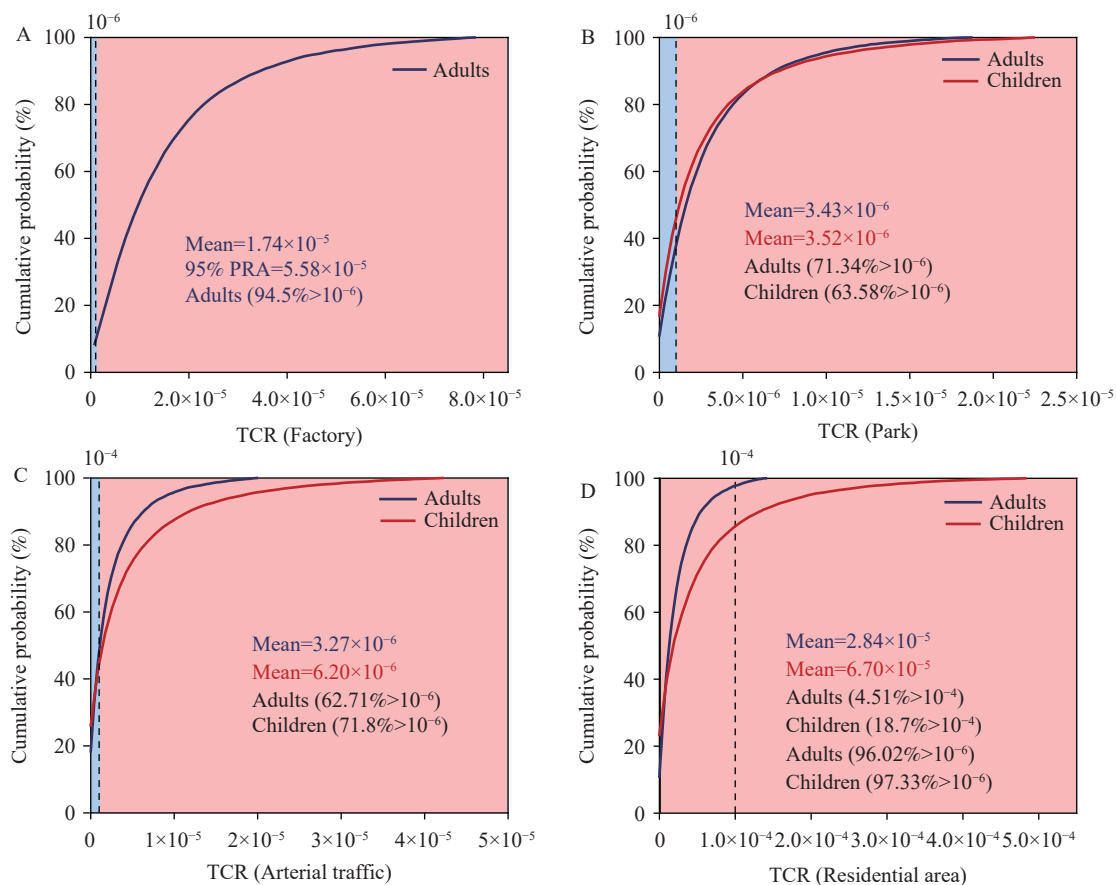


FIGURE 3. Probability distribution characteristics of total carcinogenic risk of trace metals in various microenvironments. (A) Factory; (B) Park; (C) Arterial traffic; (D) Residential area. Abbreviation: TCR=the total carcinogenic risk.

residential and industrial areas have been identified as As, Pb, and Mn.

Comparison of The Comprehensive Results of Probabilistic and Deterministic Health Risk Evaluation

Table 1 delineates the discrepancies between deterministic and probabilistic risk assessment methodologies. For instance, the deterministic assessment indicates that the CR for adults due to Pb are within the acceptable thresholds set by the USEPA. In contrast, probabilistic assessments show that the median CR from Pb exposure is 1.01×10^{-5} , surpassing the acceptable risk level. Additionally, the results from probabilistic assessments for Mn, Sb, and Hg are higher than those obtained from deterministic assessments, suggesting that deterministic methods may underrepresent the associated risks. Conversely, with As, the probabilistic method yielded higher NCR results, but lower CR compared to deterministic

assessments. Similarly, the hazard quotients for Cd and Co in adults increased under the probabilistic method, while decreasing for other elements. This variation can likely be attributed to the probabilistic method providing a more detailed analysis of the concentrations of each TM involved.

DISCUSSION

In this study, an initial deterministic risk assessment was conducted to identify high-risk pollutants. The assessment revealed that the concentrations of Co, Cd, Sb, Mn, As, Pb, and Hg pose significant risks to both adults and children. Research indicates that maternal exposure to these metal mixtures during pregnancy is linked to an increased risk of congenital heart defects, allergic disorders, and neurodevelopmental disorders in offspring (16–18). Furthermore, exposure to neurotoxic metals is associated with cognitive decline in older adults (19). Cadmium exposure has also been implicated in the onset of obesity and related metabolic

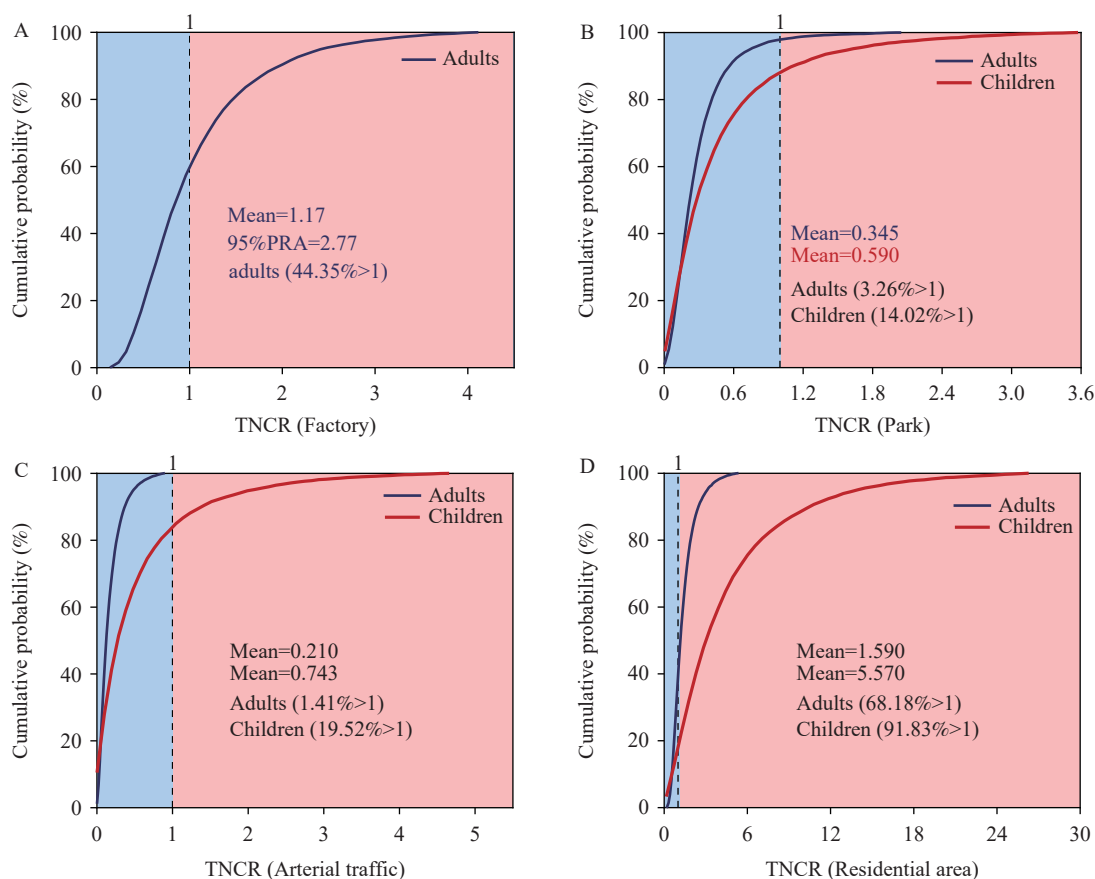


FIGURE 4. Probability distribution characteristics of total non-carcinogenic risk for trace metals in various microenvironments. (A) Factory; (B) Park; (C) Arterial traffic; (D) Residential area. Abbreviation: TNCR=the total non-carcinogenic risk.

TABLE 1. Comparison of the deterministic risk at the 50% quantile of sampling point concentrations with the 50% probability risk sum across 4 microenvironments.

| Elements | DRA | | | | PRA | | | |
|----------|-----------------------|-----------------------|-----------------------|-----------------------|-----------------------|-----------------------|-----------------------|-----------------------|
| | Adults | | Children | | Adults | | Children | |
| | CR | NCR | CR | NCR | CR | NCR | CR | NCR |
| Mn | / | 1.04 | / | 1.31 | / | 1.17 | / | 1.35 |
| Co | 3.24×10^{-6} | 2.06×10^{-1} | 1.01×10^{-6} | 3.50×10^{-1} | 1.64×10^{-6} | 2.17×10^{-1} | 4.13×10^{-7} | 3.23×10^{-1} |
| As | 2.26×10^{-5} | 4.82×10^{-1} | 2.54×10^{-5} | 1.12 | 2.11×10^{-5} | 8.34×10^{-1} | 1.86×10^{-5} | 1.84 |
| Cd | 5.84×10^{-7} | 1.09×10^{-1} | 1.83×10^{-7} | 1.65×10^{-1} | 5.04×10^{-7} | 0.22 | 6.64×10^{-8} | 0.16 |
| Sb | / | 1.28×10^{-2} | / | 7.36×10^{-2} | / | 2.70×10^{-2} | / | 1.08×10^{-1} |
| Pb | 8.13×10^{-7} | / | 1.13×10^{-6} | / | 1.01×10^{-5} | / | 1.21×10^{-5} | / |
| Hg | / | 1.59×10^{-2} | / | 5.67×10^{-2} | / | 3.47×10^{-2} | / | 1.49×10^{-1} |

Note: "/" means not applicable.

Abbreviation: DRA=deterministic risk assessment; PRA=probabilistic risk assessment; CR=carcinogenic risk; NCR=non-carcinogenic risk.

disorders (20). Additionally, elevated serum levels of lead and cadmium have been shown to negatively impact red blood cell folate levels and contribute to reproductive toxicity and the development of testicular germ cell neoplasia in situ in murine models (21–22). Given these findings, it is crucial to execute a more

precise probabilistic risk assessment for these identified high-risk pollutants.

Variables such as exposure duration and pollutant concentration can vary markedly in the dynamic settings of work and living environments, critically influencing the outcomes of risk assessments (8,23).

Regional assessments have been employed to evaluate probabilistic health risks from heavy metal exposure, considering varying exposure frequencies, routes, and land uses (24). In a study from The Republic of Korea, the health risks associated with particulate matter exposure among preschool children in Seoul were evaluated, taking into account primary microenvironments and their corresponding time-activity patterns (25). This study developed an advanced probabilistic health risk assessment model focusing on microenvironmental exposures, which pertain to pollutant exposure within specific, spatially-defined areas over time, particularly where individuals reside or interact with environmental pollutants. Findings from this microenvironment-based probabilistic health risk assessment indicated that critical areas and primary targets in residential and factory settings face the highest health risks, with As, Pb, and Mn identified as the main contaminants of concern.

Previous studies have indicated that the primary distinction lies in the supplemental data gained through probabilistic assessment. This information can be employed to implement proactive actions to mitigate current exposure. Furthermore, probabilistic assessment offers insights into the extent of exposure and the safety margin (26), providing critical guidance for soil management and remediation.

It can be concluded that using a risk assessment model tailored to specific microenvironments has significantly reduced the extent of contaminated land requiring treatment and rehabilitation. However, this approach is primarily effective for small-scale pollutant exposures. Additionally, it is challenging to delineate the contribution of various soil pollution sources to health risks. Future models for health risk assessment should consider integrating additional limiting factors, including exposure among occupational populations and soil characteristics such as type, particle size, permeability, and pH. Incorporating these factors would furnish decision-makers with more precise and critical information.

Conflicts of interest: No conflicts of interest.

doi: 10.46234/ccdcw2024.167

* Corresponding author: Qiong Wang, wangqiong@nieh.chinacdc.cn.

¹ Guangdong Provincial Key Laboratory of High-Quality Recycling of End-of-Life New Energy Devices, Guangzhou Institute of Energy Research, Chinese Academy of Sciences, Guangzhou City, Guangdong Province, China; ² State Environmental Protection Key Laboratory of Environmental Pollution Health Risk Assessment, Center for Environmental Health Research, South China Institute of

Environmental Sciences, The Ministry of Ecological and Environment of China, Guangzhou City, Guangdong Province, China; ³ Dezhou Center for Disease Control and Prevention, Dezhou City, Shandong Province, China; ⁴ School of Public Health, China Medical University, Shenyang City, Liaoning Province, China; ⁵ China CDC Key Laboratory of Environment and Population Health, National Institute of Environmental Health, Chinese Center for Disease Control and Prevention Beijing, China.

Submitted: August 27, 2023; Accepted: March 25, 2024

REFERENCES

- Liu R, Zhang H, Gou X, Luo XQ, Yang HY. Approaches of health risk assessment for heavy metals applied in China and advance in exposure assessment models: a review. *Ecol Environ Sci* 2014;23(7):1239 – 44. <https://doi.org/10.3969/j.issn.1674-5906.2014.07.023>.
- Jiménez-Oyola S, Segovia KE, García-Martínez MJ, Ortega M, Bolonio D, García-Garizabal I, et al. Human health risk assessment for exposure to potentially toxic elements in polluted rivers in the equatorial amazon. *Water* 2021;13(5):613. <https://doi.org/10.3390/w13050613>.
- Liu JW, Zhang AC, Chen YJ, Zhou X, Zhou AQ, Cao HB. Bioaccessibility, source impact and probabilistic health risk of the toxic metals in PM_{2.5} based on lung fluids test and Monte Carlo simulations. *J Cleaner Prod* 2021;283:124667. <https://doi.org/10.1016/j.jclepro.2020.124667>.
- Li F, Wang XY, Li X. Health risk assessment for heavy metals in soils and quantitative study of parameter uncertainty. *J Hunan Univ (Nat Sci)* 2015;42(6):119 – 26. <https://doi.org/10.3969/j.issn.1674-2974.2015.06.020>.
- Thompson KM, Burmaster DE, Crouch EAC. Monte Carlo techniques for quantitative uncertainty analysis in public health risk assessments. *Risk Anal* 1992;12(1):53 – 63. <https://doi.org/10.1111/j.1539-6924.1992.tb01307.x>.
- Chen HR, Wang L, Hu BF, Xu JM, Liu XM. Potential driving forces and probabilistic health risks of heavy metal accumulation in the soils from an e-waste area, southeast China. *Chemosphere* 2022;289:133182. <https://doi.org/10.1016/j.chemosphere.2021.133182>.
- Qin N, Tuexunbieke A, Wang Q, Chen X, Hou R, Xu XY, et al. Key factors for improving the carcinogenic risk assessment of PAH inhalation exposure by Monte Carlo simulation. *Int J Environ Res Public Health* 2021;18(21):11106. <https://doi.org/10.3390/ijerph182111106>.
- Donald M, Mengersen K, Toze S, Sidhu JPS, Cook A. Incorporating parameter uncertainty into quantitative microbial risk assessment (QMRA). *J Water Health* 2011;9(1):10 – 26. <https://doi.org/10.2166/wh.2010.073>.
- Xu SH, Wang LH. The interactive relationship between city innovation and the upgrading of local industrial clusters: based on Shaoguan manufacturing industry. *J Northwest Univ (Nat Sci Ed)* 2014;44(2):297 – 305. <https://doi.org/10.16152/j.cnki.xdxzbz.2014.02.033>.
- USEPA. Microwave assisted acid digestion of sediments, sludges, soils, and oils. 1998. https://synectics.net/public/library/StreamResource.axd?DSN=pub&Mode=FileImage_Inline&ID=1731. [2022-08-10].
- Liu LL, Liu QY, Ma J, Wu HW, Qu YJ, Gong YW, et al. Heavy metal (loid)s in the topsoil of urban parks in Beijing, China: concentrations, potential sources, and risk assessment. *Environ Pollut* 2020;260:114083. <https://doi.org/10.1016/j.envpol.2020.114083>.
- Cao SZ, Wen DS, Chen X, Duan XL, Zhang LL, Wang BB, et al. Source identification of pollution and health risks to metals in household indoor and outdoor dust: a cross-sectional study in a typical mining town, China. *Environ Pollut* 2022;293:118551. <https://doi.org/10.1016/j.envpol.2021.118551>.
- Matz CJ, Strieb DM, Davis K, Egyed M, Rose A, Chou B, et al. Effects of age, season, gender and urban-rural status on time-activity: Canadian human activity pattern survey 2 (CHAPS 2). *Int J Environ Res Public Health* 2014;11(2):2108 – 24. <https://doi.org/10.3390/ijerph11022108>.

- 10202108.
14. Barrio-Parra F, Izquierdo-Díaz M, Dominguez-Castillo A, Medina R, De Miguel E. Human-health probabilistic risk assessment: the role of exposure factors in an urban garden scenario. *Landscape Urban Plann* 2019;185:191 – 9. <https://doi.org/10.1016/j.landurbplan.2019.02.005>.
 15. Yu YJ, Zhu XH, Li LZ, Lin BG, Xiang MD, Zhang XH, et al. Health implication of heavy metals exposure via multiple pathways for residents living near a former e-waste recycling area in China: a comparative study. *Ecotoxicol Environ Saf* 2019;169:178 – 84. <https://doi.org/10.1016/j.ecoenv.2018.10.115>.
 16. Wang CR, Pi X, Yin SJ, Liu MY, Tian T, Jin L, et al. Maternal exposure to heavy metals and risk for severe congenital heart defects in offspring. *Environ Res* 2022;212:113432. <https://doi.org/10.1016/j.envres.2022.113432>.
 17. Ruan FY, Zhang JJ, Liu J, Sun XJ, Li YY, Xu SQ, et al. Association between prenatal exposure to metal mixtures and early childhood allergic diseases. *Environ Res* 2022;206:112615. <https://doi.org/10.1016/j.envres.2021.112615>.
 18. Yamamoto M, Eguchi A, Sakurai K, Nakayama SF, Sekiyama M, Mori C, et al. Longitudinal analyses of maternal and cord blood manganese levels and neurodevelopment in children up to 3 years of age: the Japan environment and children's study (JECS). *Environ Int* 2022;161:107126. <https://doi.org/10.1016/j.envint.2022.107126>.
 19. Sasaki N, Carpenter, D.O. Associations between Metal Exposures and Cognitive Function in American Older Adults. *Int. J. Environ. Res. Public Health* 2022, 19, 2327. <https://doi.org/10.3390/ijerph19042327>
 20. Gasser M, Lenglet S, Bararpour N, Sajic T, Wiskott K, Augsburg M, et al. Cadmium acute exposure induces metabolic and transcriptomic perturbations in human mature adipocytes. *Toxicology* 2022;470:153153. <https://doi.org/10.1016/j.tox.2022.153153>.
 21. Mitra S, Patra T, Saha D, Ghosh P, Mustafi SM, Varghese AC, et al. Sub-chronic cadmium and lead compound exposure induces reproductive toxicity and development of testicular germ cell neoplasia in situ in murine model: attenuative effects of resveratrol. *J Biochem Mol Toxicol* 2022;36(7):e23058. <https://doi.org/10.1002/jbt.23058>.
 22. Wang BK, Chen WL. Detrimental health relationship between blood lead and cadmium and the red blood cell folate level. *Sci Rep* 2022;12(1):6628. <https://doi.org/10.1038/s41598-022-10562-9>.
 23. Biesiada M. Simulations in health risk assessment. *Int J Occup Med Environ Health* 2001;14(4):397-402. <https://pubmed.ncbi.nlm.nih.gov/11885924/>.
 24. Peng C, Cai YM, Wang TY, Xiao RB, Chen WP. Regional probabilistic risk assessment of heavy metals in different environmental media and land uses: an urbanization-affected drinking water supply area. *Sci Rep* 2016;6(1):37084. <https://doi.org/10.1038/srep37084>.
 25. Jeong K, Hong J, Lee Y, Yang J, Lim Y, Shin D, et al. Risk assessment of particulate matter by considering time-activity-pattern and major microenvironments for preschool children living in Seoul, south Korea. *Environ Sci Pollut Res* 2021;28(28):37506 – 19. <https://doi.org/10.1007/s11356-021-13106-2>.
 26. Sander P, Öberg T. Comparing deterministic and probabilistic risk assessments. A case study at a closed steel mill in southern Sweden (7 pp). *J Soils Sediments* 2006;6(1):55 – 61. <https://doi.org/10.1065/jss2005.10.147>.

SUPPLEMENTARY MATERIAL

Human health risk assessment model: Human health risks, encompassing both carcinogenic risks (CR) and non-carcinogenic risks (NCR), were evaluated using the following health risk calculation model:

The average daily intake (ADI) in mg/(kg·day) was calculated using Equations 1 to 3, as recommended by the USEPA (2001).

$$ADI_{ing} = \frac{IR_{ing} \times EF \times ED}{BW \times AT} \times 10^{-6} \quad (1)$$

$$ADI_{dermal} = \frac{SAE \times AF \times ABS \times EF \times ED}{BW \times AT} \times 10^{-6} \quad (2)$$

$$ADI_{inh} = \frac{IR_{inh} \times EF \times ED \times PM}{BW \times AT} \times 10^{-6} \quad (3)$$

Where IR is the ingestion rate (kg/day), EF is the frequency of exposure (day/year), ED is the exposure duration (year), BW is the body weight (kg), and AT is the average lifetime of days (day). SAE is the surface area of the exposed skin (cm²), AF is the adherence factor (mg/cm²-day), and ABS is the dermal absorption factor (unitless). PM is the content of inhalable particulates in ambient air (mg/m³).

The CR assessment: The CR and the total carcinogenic risk (TCR) were calculated by Equations 4 and 5

$$CR_i = ADI_{ing} \times C_i \times SF_{ing} + ADI_{dermal} \times C_i \times SF_{dermal} + ADI_{inh} \times C_i \times SF_{inh} \quad (4)$$

$$TCR = \sum CR_i \quad (5)$$

Where CR represents the carcinogenic risk posed by the ith heavy metals in soil, TCR denotes the total carcinogenic risk from heavy metals in soil, and SF refers to the carcinogenic slope factor (kg·day/mg). C signifies the concentration of the heavy metal in a specific exposure medium (mg/kg).

The NCR assessment: The NCR and the total non-carcinogenic risk (TNCR) were calculated by Equation 6

$$NCR_i = \frac{ADI_{ing} \times C_i}{RfD_{ing}} + \frac{ADI_{dermal} \times C_i}{RfD_{dermal}} + \frac{ADI_{inh} \times C_i}{RfD_{inh}} \quad (6)$$

SUPPLEMENTARY TABLE S1. Toxicological data for heavy metals.

| Elements | RfD _{ing} | RfD _{dermal} | RfD _{inh} | SF _{ing} | SF _{inh} | ABS | SF _{dermal} |
|------------------|-----------------------|-----------------------|-----------------------|-----------------------|-----------------------|-----------------------|-----------------------|
| Be | 2.00×10 ⁻³ | 1.40×10 ⁻⁵ | 4.69×10 ⁻⁶ | / | 10.20 | / | |
| Cr ³⁺ | 1.5 | 1.95×10 ⁻² | | / | | 0.10 | |
| Mn | 0.14 | 0.14 | 1.17×10 ⁻⁵ | / | | / | |
| Co | 3.00×10 ⁻⁴ | 3.00×10 ⁻⁴ | 1.41×10 ⁻⁶ | / | 38.40 | / | |
| Ni | 2.00×10 ⁻² | 8.00×10 ⁻⁴ | 2.11×10 ⁻⁵ | / | 1.11 | 9.10×10 ⁻² | |
| Cu | 4.00×10 ⁻² | 4.00×10 ⁻² | | / | | 6.00×10 ⁻² | |
| Zn | 0.30 | 3.00×10 ⁻¹ | | / | | 0.10 | |
| As | 3.00×10 ⁻⁴ | 3.00×10 ⁻⁴ | 3.52×10 ⁻⁶ | 1.50 | 18.30 | 3.00×10 ⁻² | 1.5 |
| Mo | 5.00×10 ⁻³ | 5.00×10 ⁻³ | 4.69×10 ⁻⁴ | / | | 1.00×10 ⁻² | |
| Ag | 5.00×10 ⁻³ | 2.00×10 ⁻⁴ | | / | | / | |
| Cd | 1.00×10 ⁻³ | 2.50×10 ⁻⁵ | 2.35×10 ⁻⁶ | / | 7.67 | 1.00×10 ⁻³ | |
| Sn | 0.60 | 0.60 | | / | | / | |
| Sb | 4.00×10 ⁻⁴ | 6.00×10 ⁻⁵ | 7.04×10 ⁻⁵ | / | | / | |
| Tl | 1.00×10 ⁻⁵ | 1.00×10 ⁻⁵ | | / | | / | |
| Pb | / | | | 8.50×10 ⁻³ | 5.11×10 ⁻² | 6.00×10 ⁻³ | 8.50×10 ⁻³ |
| Hg | 3.00×10 ⁻⁴ | 2.10×10 ⁻⁵ | 7.04×10 ⁻⁵ | / | | 1.00 | |

Note: "/" means not applicable. Subscripts ing, inh, and dermal represent ingestion, inhalation, and dermal contact pathways, respectively. Abbreviation: RfD=the reference dose; SF=the carcinogenic slope factor; ABS=the dermal absorption factor.

$$TNCR = \sum NCR_i \quad (7)$$

Where RfD denotes the reference dose [mg/(kg·day)] for a heavy metal via a specific absorption pathway; TNCR signifies the total aggregate NCR presented by all heavy metals in soil.

SUPPLEMENTARY TABLE S2. Pollutant concentration.

| Elements | The mean | The standard deviation | The maximum | The minimum | 5% | 50% | 95% |
|----------|-----------|------------------------|-------------|-------------|--------|--------|-----------|
| Be | 1.36 | 0.63 | 3.10 | 0.39 | 0.46 | 1.25 | 2.39 |
| Cr | 40.53 | 33.98 | 192.00 | 10.20 | 13.33 | 34.05 | 86.19 |
| Mn | 588.22 | 522.07 | 2,740.00 | 75.20 | 132.60 | 454.00 | 1,337.80 |
| Co | 11.91 | 6.81 | 29.90 | 3.33 | 4.33 | 10.00 | 25.98 |
| Ni | 1.02 | 0.58 | 2.70 | 0.41 | 0.43 | 0.44 | 2.07 |
| Cu | 176.46 | 447.62 | 1,929.00 | 9.51 | 12.44 | 45.30 | 1,119.35 |
| Zn | 1,669.85 | 3,471.78 | 16,286.00 | 69.10 | 79.35 | 518.00 | 5,534.40 |
| As | 120.71 | 206.51 | 860.00 | 10.40 | 16.25 | 49.50 | 610.05 |
| Mo | 6.24 | 18.06 | 97.10 | 0.07 | 0.48 | 1.50 | 10.92 |
| Ag | 13.13 | 10.63 | 43.50 | 1.56 | 2.41 | 5.30 | 24.98 |
| Cd | 52.21 | 161.66 | 862.00 | 0.55 | 0.87 | 9.00 | 123.55 |
| Sn | 18.85 | 54.25 | 280.00 | 0.64 | 0.79 | 4.66 | 46.12 |
| Sb | 63.65 | 183.38 | 779.00 | 0.58 | 1.52 | 8.27 | 464.31 |
| Tl | 2.85 | 10.10 | 52.20 | 0.10 | 0.13 | 0.35 | 2.58 |
| Pb | 17,325.15 | 34,677.33 | 97,900.00 | 102.00 | 140.00 | 870.50 | 96,000.00 |
| Hg | 20.30 | 92.20 | 499.00 | 0.07 | 0.15 | 1.03 | 14.87 |

SUPPLEMENTARY TABLE S3. Recommended values for deterministic risk assessment.

| Parameter | Description | Unit | Recommended value | | Reference |
|---------------|--|-------------------------|--|--------|-----------------------------|
| | | | Children | Adults | |
| EF | exposure frequency | day/year | 350 | | USEPA, 2011 |
| IR_{ingest} | ingestion rate of soil | mg/day | 103 | 30 | Yang et al. 2019 |
| BW | average body weight | kg | 29.3 | 61.8 | Huang et al. 2020 |
| AF | skin adherence factor | mg/cm ² -day | 0.2 | 0.07 | USEPA, 2011 |
| SAE | exposed skin area | cm ² | 2,800 | 5,256 | Duan et al. 2013 |
| IR_{inhal} | Inhalation rate | m ³ /day | 8.6 | 14.5 | MEP 2014, Huang et al. 2020 |
| ED | exposure duration | years | 6 | 24 | MEP 2014 |
| PM | Content of inhalable particulates in ambient air | µg/m ³ | 0.119 | 0.119 | USEPA, 2011 |
| AT | average time of exposure to contaminated soils | day | 365*ED (non-carcinogenic) 365*76 (carcinogenic) | | MEP 2013 |

Abbreviation: EF=exposure frequency; IR_{ingest} =ingestion rate; BW=body weight; AF=skin adherence factor; SAE=skin area; IR_{inhal} =inhalation rate; ED=exposure duration; PM=particulates in ambient air; AT=average time.

SUPPLEMENTARY TABLE S4. Calculation parameters and values used in a health risk assessment model to evaluate exposure risks of soil using a Monte Carlo simulator.

| Parameter | Description | Unit | Type | Residential quarter, park, arterial traffic | | Factory |
|---------------|--|-------------------------|------------------------|--|-----------------------|-----------------------|
| | | | | Children | Adults | Adult |
| EF | exposure frequency | day/year | Triangular* | TRI* (180,350,365) | | TRI (225,250,300) |
| IR_{ingest} | ingestion rate of soil | mg/day | Triangular | TRI (66,103,161) | TRI (4,30,52) | TRI (4,30,52) |
| BW | average body weight | Kg | Lognormal [†] | LN (28.99, 21.13) | LN (60.37, 10.34) | LN (60.37, 10.34) |
| AF | skin adherence factor | mg/cm ² -day | Beta-PERT [§] | 0.2 (0, 3.3) | 0.07 (0,0.3) | 0.2 (0, 3.3) |
| SAE | exposed skin area | cm ² | / | TRI (900,2030,7000) | LN (5,272.84, 529.37) | LN (2,965.97, 297.77) |
| IR_{inhal} | Inhalation rate | m ³ /day | Lognormal | LN (10.24, 3.84) | LN (14.34, 2.18) | LN (14.34, 2.18) |
| ED | exposure duration | Years | Uniform | (0, 6) | (0, 24) | (0, 25) |
| PM | Content of inhalable particulates in ambient air | mg/m ³ | Point | 0.119 | | |
| AT | average time of exposure to contaminated soils | Day | Point | 365*ED (non-carcinogenic) 365*76 (carcinogenic) | | |

Note: "/" means not applicable.

Abbreviation: TRI=triangular; LN=lognorma; EF=exposure frequency; IR_{ingest} =ingestion rate; BW=body weight; AF=skin adherence factor; SAE=skin area; IR_{inhal} =inhalationrate; ED=exposure duration; PM=particulates in ambient air; AT=average time.

* For TRI, the likeliest (minimum–maximum) for the triangular distribution.

[†] For LN, (average, standard deviation) for the Lognormal distribution.

[§] Likeliest (minimum–maximum) for the Beta-PERT distribution.

SUPPLEMENTARY TABLE S5. Uncertain concentrations (mg/kg) of heavy metalloids in soils across various microenvironments.

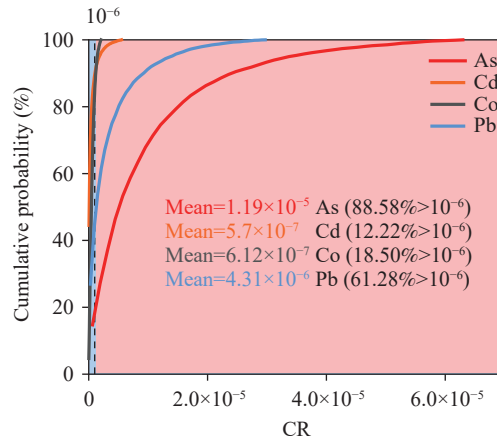
| Elements | Probabilistic distribution | Parameters (log μ , log σ) | | | |
|----------|----------------------------|--|------------|------------------|---------------------|
| | | Factory | Park | Arterial traffic | Residential quarter |
| Mn | Lognormal | 6.14, 0.95 | 6.14, 0.54 | 6.08, 0.81 | 6.03, 0.54 |
| Co | Lognormal | 2.51, 0.53 | 2.25, 0.57 | 2.40, 0.56 | 2.11, 0.51 |
| As | Lognormal | 4.26, 0.88 | 3.90, 0.70 | 4.42, 1.17 | 4.02, 1.07 |
| Cd | Lognormal | 3.04, 1.50 | 1.99, 2.11 | 2.12, 1.84 | 1.10, 2.06 |
| Sb | Lognormal | 2.05, 2.44 | 1.43, 1.99 | 2.53, 1.98 | 2.09, 1.48 |
| Pb | Lognormal | 9.10, 1.21 | 8.16, 1.47 | 9.23, 1.19 | 9.22, 1.22 |
| Hg | Lognormal | 1.15, 1.80 | 0.38, 1.24 | 0.20, 2.05 | -0.57, 1.16 |

SUPPLEMENTARY TABLE S6. Exposure parameters for receptor population groups in contact with soils from varied land uses.

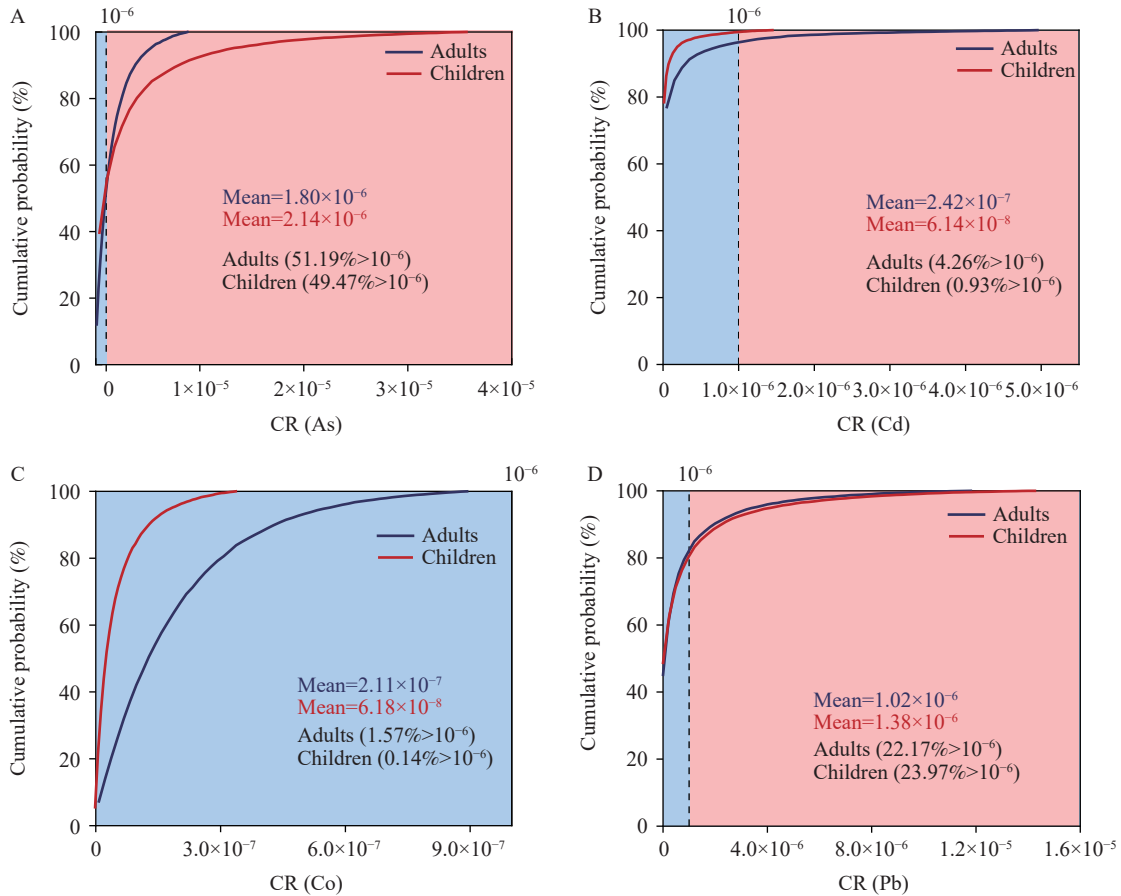
| Microenvironment | The crowd | Number | ET (h/24) |
|---------------------|-----------|--------|---------------------|
| | | | Triangular* |
| Factory | Adults | 56 | 8.00 (7.20–10.00) |
| | Children | 76 | 2.80 (0.07–7.00) |
| Park | Adults | 47 | 1.08 (0.29–3.75) |
| | Children | 75 | 0.96 (0.07–3.25) |
| Arterial traffic | Adults | 216 | 1.00 (0.07–2.70) |
| | Children | 200 | 18.40 (9.75–23.25) |
| Residential quarter | Adults | 245 | 17.70 (12.40–23.70) |
| | Children | | |

Note: Adults assess the health risks associated with factories, parks, and major traffic routes; however, children's risk assessments do not typically include factories and are influenced by specific circumstances.

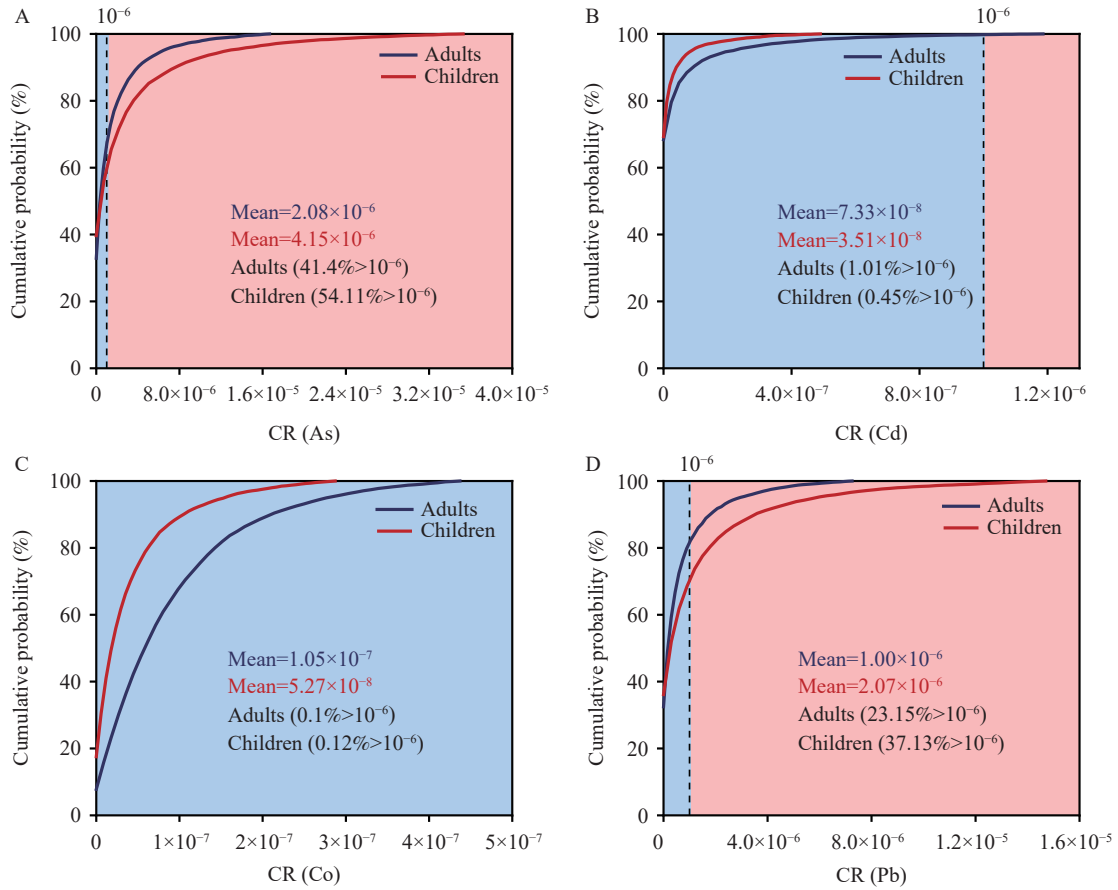
* for the likeliest (minimum–maximum) for the triangular distribution.



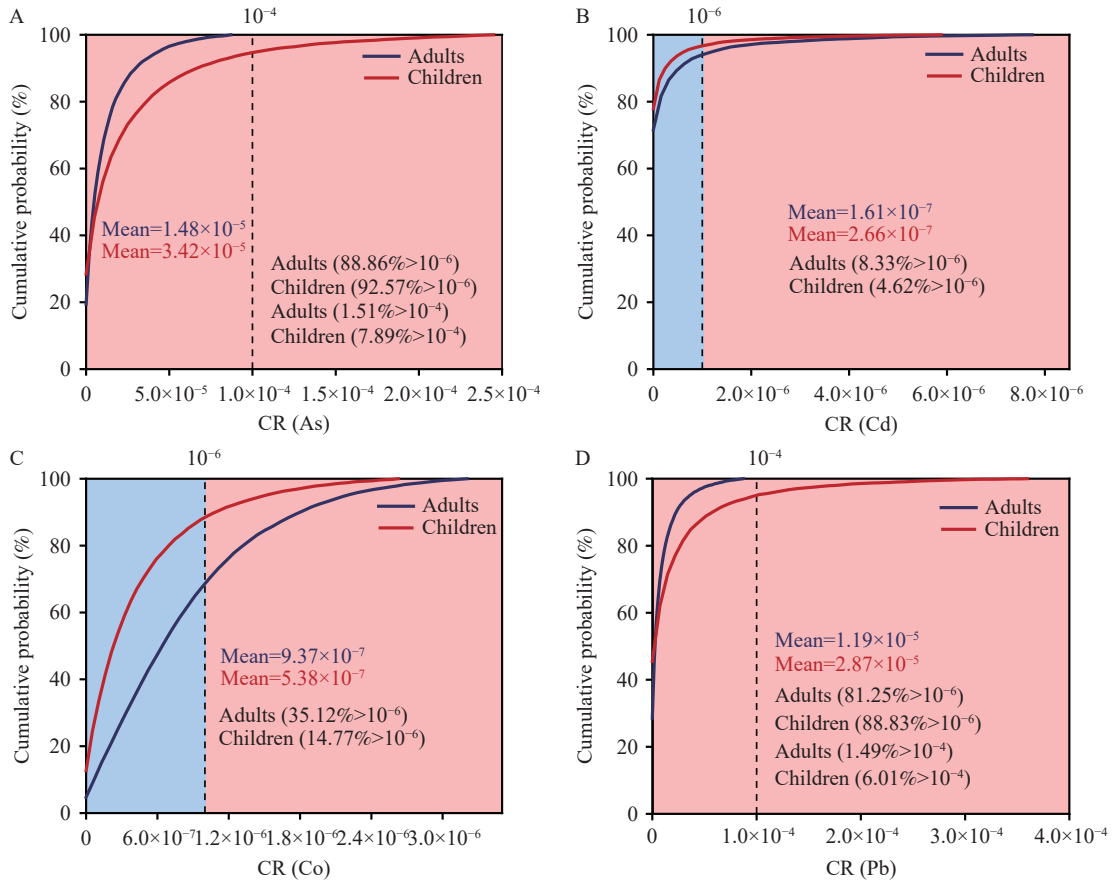
SUPPLEMENTARY FIGURE S1. CR results from probabilistic risk assessment in a factory microenvironment. Abbreviation: CR=carcinogenic risk.



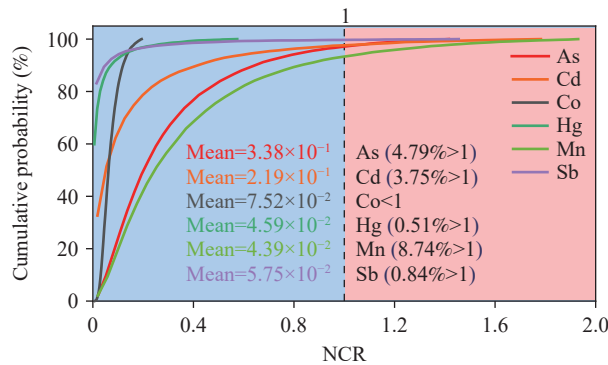
SUPPLEMENTARY FIGURE S2. CR results from probabilistic risk assessment in a park microenvironment. (A) CR for As; (B) CR for Cd; (C) CR for Co; (D) CR for Pb. Abbreviation: CR=carcinogenic risk.



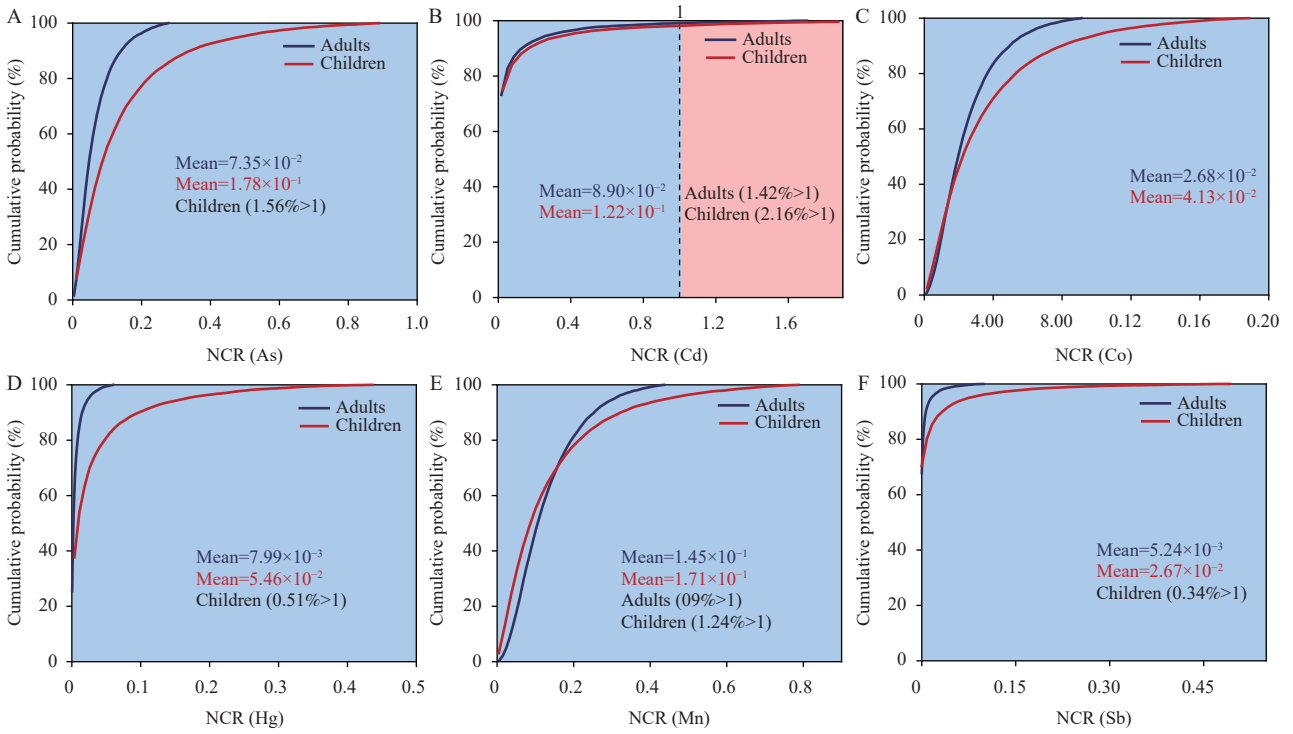
SUPPLEMENTARY FIGURE S3. CR outcomes from probabilistic risk assessments in arterial traffic microenvironments. (A) CR for As; (B) CR for Cd; (C) CR for Co; (D) CR for Pb. Abbreviation: CR=carcinogenic risk.



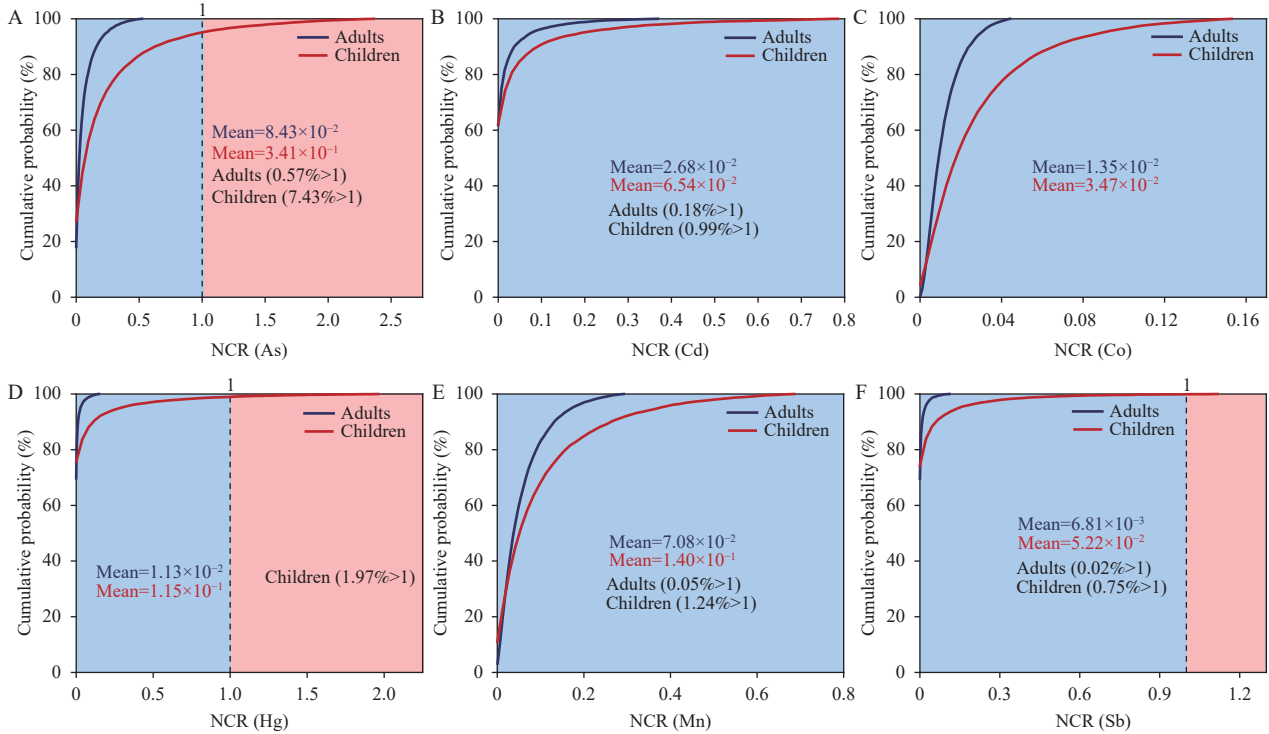
SUPPLEMENTARY FIGURE S4. CR results from probabilistic risk assessment in residential quarter microenvironments. (A) CR for As; (B) CR for Cd; (C) CR for Co; (D) CR for Pb. Abbreviation: CR=carcinogenic risk.



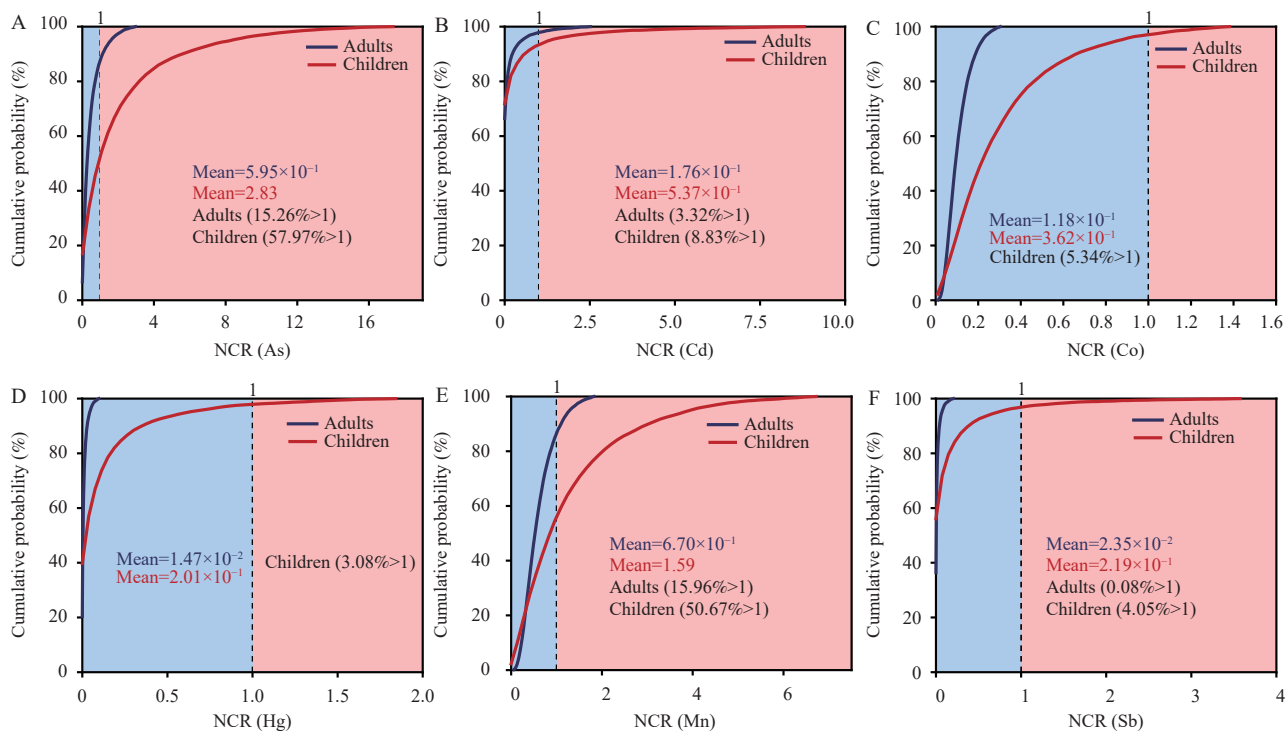
SUPPLEMENTARY FIGURE S5. NCR results from probabilistic risk assessment in the factory microenvironment. Abbreviation: NCR=non-carcinogenic risk.



SUPPLEMENTARY FIGURE S6. NCR results from probabilistic risk assessment in a park microenvironment. (A) NCR for As; (B) NCR for Cd; (C) NCR for Co; (D) NCR for Hg; (E) NCR for Mn; (F) NCR for Sb. Abbreviation: NCR=non-carcinogenic risk.



SUPPLEMENTARY FIGURE S7. NCR results from a probabilistic risk assessment in the arterial traffic microenvironment. (A) NCR for As; (B) NCR for Cd; (C) NCR for Co; (D) NCR for Hg; (E) NCR for Mn; (F) NCR for Sb. Abbreviation: NCR=non-carcinogenic risk.



SUPPLEMENTARY FIGURE S8. NCR results from probabilistic risk assessment in residential quarter microenvironments. (A) NCR for As; (B) NCR for Cd; (C) NCR for Co; (D) NCR for Hg; (E) NCR for Mn; (F) NCR for Sb. Abbreviation: NCR=non-carcinogenic risk.